Elasto-optic coefficients of $Sn_2P_2S_6$ crystals as determined with Dixon-Cohen method

[1] Martynyuk-Lototska I., [1] Dudok T., [1] Mys O., [2] Grabar A. and [1] Vlokh R.

[1] Vlokh Institute of Physical Optics, 23 Dragomanov Street, 79005, Lviv, Ukraine
[2] Uzhhorod National University, 54 Voloshyn Street, 88000, Uzhhorod, Ukraine

Received: 07.03.2019

Abstract. Using a Dixon-Cohen method, a set of elasto-optic coefficients and the corresponding acousto-optic figures of merit are determined for $Sn_2P_2S_6$ crystals. We consider diffraction geometry associated with acousto-optic interactions that involve purely longitudinal acoustic wave propagating along the crystallographic axis *b*. It is found that the maximal acousto-optic figure of merit for this geometry, $(447\pm10)\times10^{-15}$ s^3/kg, is achieved in the case of isotropic interactions with the optical wave polarized parallel to the *b* axis.

Keywords: elasto-optic coefficients, acousto-optic diffraction, $Sn_2P_2S_6$ crystals

UDC: 535.42

1. Introduction

Tin thiohypodiphosphate, $Sn_2P_2S_6$, represents a wide-bandgap semiconductor with a proper second-order paraelectric-to-ferroelectric phase transition $2/m \leftrightarrow m$ occurring at $T_C = 337$ K [1]. The crystal is transparent in a wide spectral interval ranging from $\lambda = 0.53$ μm to $\lambda = 8.0$ μm [2]. $Sn_2P_2S_6$ possesses large enough electrooptic coefficients ($r_{11} = 1.74\times10^{-10}$ m/V [2, 3]) and Verdet constant (115 rad/T×m) [4] at the room temperature and the light wavelength $\lambda = 632.8$ nm. Recently we have shown [5–7] that acousto-optic (AO) figure of merit M_2 for the $Sn_2P_2S_6$ crystals can reach very high values, $M_2 = (1.7\pm0.4)\times10^{-12}$ s^3/kg^2, for the case of AO interactions with a quasi-transverse acoustic wave. Notice that the other crystals of this family, in particular $Pb_2P_2Se_6$, are also expected to be efficient AO materials [6].

It is known that $Sn_2P_2S_2$ possesses a photorefractive effect in the visible spectral range [7, 8]. As a result, the crystals of its family can be applied in AO devices designed for the infrared spectral range. Of course, any AO applications imply the knowledge of, at least, their refractive, acoustic and elasto-optic (EO) properties. The elastic properties of $Sn_2P_2S_6$ have earlier been studied in our work [9], whereas their refractive parameters can be found in Ref. [10]. At the same time, the EO characteristics have not been studied yet. In the present work we determine experimentally some of the EO coefficients for the $Sn_2P_2S_6$ crystals.

2. Experimental procedures

Single crystals of $Sn_2P_2S_6$ were grown using a vapour-transport method [11]. Single crystalline samples were oriented using an X-ray diffraction method and prepared in the shape of parallelepipeds. Since $Sn_2P_2S_6$ belongs to the monoclinic point group *m*, its crystallographic coordinate system is not orthogonal. All tensorial properties of the crystals belonging to low-symmetry groups are usually written in the Cartesian coordinate system associated with the crystallographic system. Further on, we will use a Cartesian coordinate system *XYZ* associated

with the crystallographic coordinate system *abc* as shown in Fig. 1. According to the adopted conventions, the *Y* axis of this coordinate system is orthogonal to the symmetry plane and parallel to the *b* axis. The *X* axis is directed almost along the spontaneous polarization vector, being nearly parallel to the crystallographic axis *a*. Notice that the only axis *Y* of the crystallographic coordinate system coincides with the corresponding principal axis of the optical indicatrix, while the other optical-indicatrix axes at the room temperature and the light wavelength of 632.8 nm are rotated by ~ 45 deg with respect to the *X* and *Z* axes in the *XZ* plane.

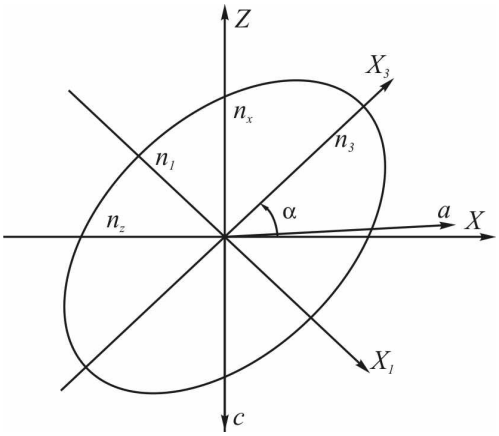

Fig. 1. Orientation of crystallographic axes *a*, *b* and *c*, along with the axes of Cartesian coordinate system *XYZ* (or the axes of refractive index ellipsoid).

All the experimental measurements were performed on single-domain samples. To reach a uniformly poled state, the samples were heated above the phase transition point ~370 K, annealed at ~350 K for about 1 h and then slowly cooled down in the external electric field ~600 V/cm applied along the *X* axis.

The EO properties were studied with a known Dixon–Cohen technique [12]. It is based on the comparison of AO parameters of a material under study with some standard (or reference) AO parameters. In our case, we used the parameters known for fused quartz. A scheme of our experimental setup is presented in Fig. 2. The sample was glued onto AO cell made from a standard

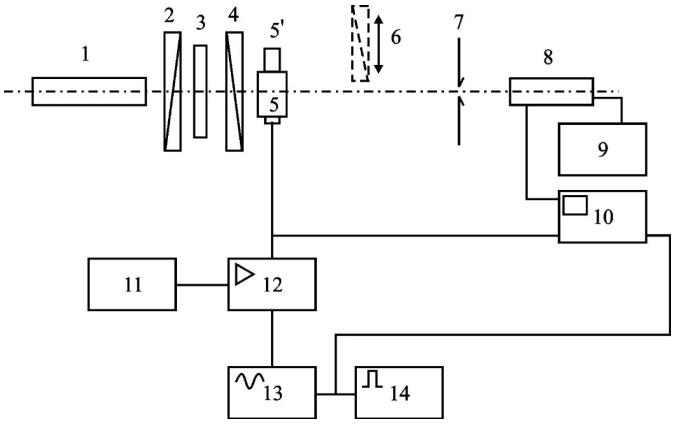

Fig. 2. Experimental setup used for measuring EO coefficients: 1 – He–Ne laser (λ=632.8 nm); 2, 4 and 6 – polarizers; 3 – λ/4 phase plate; 5 and 5' – respectively standard sample and sample under test; 7 – diaphragm; 8 – Hamamatsu S6468 photodetector with preamplifier, 9 – power supply; 10 – Silent SDS 1202X-E oscilloscope; 11 – power supply; 12 – high-frequency amplifier; 13 – high-frequency generator; 14 – SDG 2122X pulse generator.

material, i.e. fused quartz. The acoustic wave in this cell was excited by a piezoelectric transducer fabricated from $LiNbO_3$ crystals. The excited wave with the frequency $f_A = 50$ MHz was modulated by square pulses with the duration 0.5 μs and the repetition rate 300 μs.

The AO figure of merit M_2 of a sample under test can be calculated as

$$M_2^{sa} = M_2^{st} \frac{I_{st}}{I_{sa}} \left(\frac{I_3 I_4}{I_1 I_5} \right)^{1/2}, \quad (1)$$

where $M_2^{st} = 1.56 \times 10^{-15}$ s^3/kg is the reference parameter taken for the case of diffraction on the longitudinal acoustic wave [13], I_{sa} and I_{st} are the light intensities transmitted respectively through the studied and standard samples. Here the intensities of Bragg diffraction involved in Eq. (1) correspond to the interactions with forward-propagating acoustic pulse in the standard sample (I_1), forward-propagating (I_3) and reflected (I_4) pulses in the sample under study and the pulse reflected from the interface between the standard sample and the sample under study (I_5).

The experiments were carried out on the sample with parallelepiped shape, which had its faces perpendicular to the *X*, *Y* and *Z* axes. The longitudinal acoustic wave propagated along the *Y* axis. The incident light propagated along the *X* (or *Z* axes), with the polarization parallel to *Z* and *Y* axes or the directions ±45 deg with respect to the *Z* axis, (or *X* and *Y* axes or the directions ±45 deg with respect to the *X* axis). The effective EO coefficient was calculated using the relation

$$|p_{eff}| = \frac{\sqrt{M_2^{sa} \rho v_{22}^3}}{n^3}, \quad (2)$$

where *n* means the refractive index corresponding to a given light polarization, $\rho = 3560$ kg/m^3 the crystal density, and $v_{22} = 3210$ m/s the velocity of the purely longitudinal acoustic wave propagating along the *Y* direction.

3. Results and discussion

The EO and AO characteristics typical for different geometries of AO diffraction are illustrated in Table 1.

Table 1. AO and EO parameters of $Sn_2P_2S_6$ crystals and the appropriate interaction geometries.

Interaction geometry	Direction of light propagation	Direction of light polarization	n	M_2, 10^{-15} s^3/kg	p_{eff}
1	*Z*	*X*	$n_X = 3.0629$	98.3	0.118
2	*Z*	*Y*	$n_Y = 2.9309$	437.2	0.285
3	*Z*	45 deg with respect to *X* and *Y* axes	2.9950	158.0	0.161
4	*Z*	45 deg with respect to *X* and –*Y* axes	2.9950	237.8	0.197
5	*X*	*Z*	$n_Z = 3.0588$	182.1	0.162
6	*X*	*Y*	$n_Y = 2.9309$	456.6	0.291
7	*X*	45 deg with respect to *Y* and *Z* axes	2.9929	356.0	0.242
8	*X*	45 deg with respect to –*Y* and *Z* axes	2.9929	409.3	0.259

The type (1) of diffraction is implemented in the interaction plane *YZ* (see Fig. 3a). The appropriate refractive indices n_X and n_Z are as follows:

$$n_X = \left(\frac{\sin^2 \alpha}{n_1^2} + \frac{\cos^2 \alpha}{n_3^2} \right)^{-1/2}, \; n_X = \left(\frac{\cos^2 \alpha}{n_1^2} + \frac{\sin^2 \alpha}{n_3^2} \right)^{-1/2}, \; n_Y = n_2, \tag{3}$$

where α is the angle between the *X* axis and the axis of the largest principal refractive index ($\alpha = 43.3 \pm 0.4$ deg at $\lambda = 632.8$nm), whereas $n_1 = 3.0256$, $n_2 = 2.9309$ and $n_3 = 3.0982$ are the principal refractive indices measured at $\lambda = 632.8$nm [10]. For this type of interaction, the effective EO coefficient can be written as $p_{eff} = |p_{12}|$. Then we have $|p_{12}| = 0.118$. For the type (5) of diffraction taking place in the *XY* interaction plane (see Fig. 3b), the effective EO coefficient amounts to $p_{eff} = |p_{32}|$. In this case we obtain $|p_{32}| = 0.162$. The two interaction geometries given by the types (2) and (6) allow one to determine the EO tensor component p_{22}. Here the effective EO coefficient is equal to $|p_{22}| = 0.288 \pm 0.003$. The corresponding AO figure of merit is $(447 \pm 10) \times 10^{-15}$ s^3/kg. Notice that this is the highest AO figure of merit typical for the AO interactions that involve the longitudinal acoustic wave v_{22}.

The effective EO coefficient found for the types (3) and (4) of interactions is given by

$$p_{eff} = \frac{1}{4}\left(3(p_{12} + p_{22}) - (p_{11} + p_{21})\right). \tag{4}$$

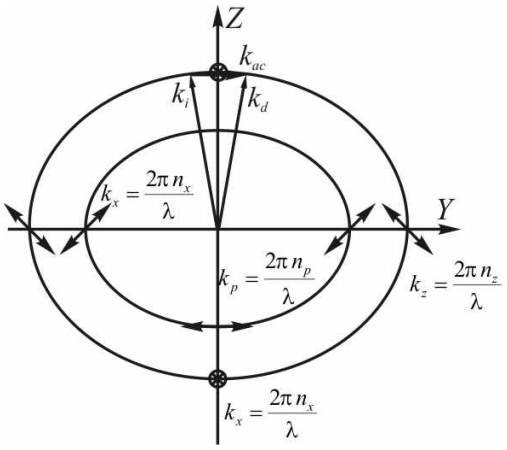

(a)

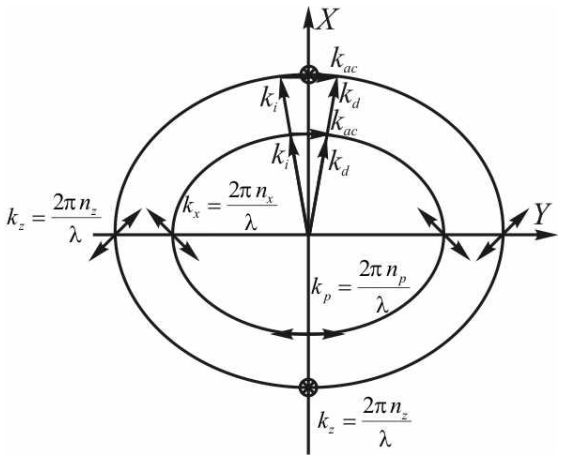

(b)

Fig. 3. Schematic vector diagrams for the AO interactions in *YZ* (a) and *XY* (b) planes.

The magnitude of this coefficient is equal to $|p_{eff}| = 0.179 \pm 0.018$. The corresponding AO figure of merit amounts to $(198 \pm 40) \times 10^{-15}$ s^3 / kg. Unfortunately, we cannot determine the combined coefficient $p_{11} + p_{21}$, since the signs of the p_{22} and p_{12} coefficients are not determined yet. Finally, the effective EO coefficient for the interaction types (7) and (8) reads as

$$p_{eff} = \frac{1}{4}\left(3(p_{32} + p_{22}) - (p_{33} + p_{23})\right). \quad (5)$$

It is equal to $|p_{eff}| = 0.251 \pm 0.009$. The corresponding AO figure of merit is very high, reaching the value $(383 \pm 27) \times 10^{-15}$ s^3/kg.

When evaluating the effective EO coefficients for the other interaction geometries and the case of interactions with quasi-transverse acoustic waves, one faces the difficulties related to insufficient sensitivity of our detection system, which cannot detect the diffraction order I_5 against the background of noises. On the other hand, we observe splitting of the Bragg diffraction maximum into a number of diffraction orders with increasing acoustic power. This is due to a high AO efficiency of $Sn_2P_2S_6$ crystals.

4. Conclusion

In this work we have determined the EO coefficients and the AO figures of merit for the $Sn_2P_2S_6$ crystals, using the standard Dixon–Cohen method. This has been done for the case of AO interactions with the purely longitudinal acoustic wave propagating along the crystallographic axis *b*. We have found that the EO coefficients are equal to $|p_{12}| = 0.118$, $|p_{32}| = 0.162$ and $|p_{22}| = 0.288 \pm 0.003$. Besides, we have determined the following values of the combined EO coefficients: $\left|\frac{1}{4}\left(3(p_{12} + p_{22}) - (p_{11} + p_{21})\right)\right| = 0.179 \pm 0.0018$ and $\left|\frac{1}{4}\left(3(p_{32} + p_{22}) - (p_{33} + p_{23})\right)\right| = 0.251 \pm 0.009$. The highest AO figure of merit reached at the interactions with the longitudinal acoustic wave propagating along the *b* axis is equal to $(447 \pm 10) \times 10^{-15}$ s^3/kg. It is achieved in the case of isotropic AO diffraction and light polarization parallel to the *b* axis. We have also observed a very high AO figure of merit typical for the interactions with the optical wave propagating along the *X* axis and polarized under the angle 45 deg with respect to the *Y* and *Z* axes. It reaches the value $(383 \pm 27) \times 10^{-15}$ s^3/kg.

References

1. Vysochanskii Yu M, Janssen T, Currat R, Folk R, Banys J, Grigas J and Samulionis V. Phase transitions in ferroelectric phosphorous chalcogenide crystals. Vilnius: Vilnius University Publishing House (2006).
2. Vlokh R O, Vysochanskii Yu M, Grabar A A, Kityk A V and Slivka V Yu, 1991. Electrooptic effect in $Sn_2P_2S_6$ ferroelectrics. Izv. Akad. Nauk SSSR, Ser. Neorg. Mater. **27**: 689–692.
3. Haertle D, Caimi G, Haldi A, Montemezzani G, Günter P, Grabar A A, Stoika I M and Vysochanskii Yu M, 2003. Electro-optical properties of $Sn_2P_2S_6$. Opt. Commun. **215**: 333–343.
4. Krupych O, Adamenko D, Mys O, Grabar A and Vlokh R, 2008. Faraday effect in $Sn_2P_2S_6$ crystals. Appl. Opt. **47**: 6040–6045.
5. Martynyuk-Lototska I Yu, Mys O G, Grabar A A, Stoika I M, Vysochanskii Yu M and Vlokh R O, 2008. Highly efficient acousto-optic diffraction in $Sn_2P_2S_6$ crystals. Appl. Opt. **47**: 52–55.
6. Martynyuk-Lototska I, Mys O, Zapeka B, Kostyrko M, Grabar A and Vlokh R, 2014. Acoustic

and elastic anisotropy of acousto-optic $Pb_2P_2Se_6$ crystals. Appl. Opt. **53**: B103–B109.
7. Odoulov S G, Shumelyuk A N, Hellwig U, Rupp R, Grabar A A and Stoyka I M, 1996. Photorefraction in tin hypothiodiphosphate in the near infrared. J. Opt. Soc. Amer. B. **13**: 2352–2360.
8. Jazbinsek M, Montemezzani G, Gunter P, Grabar A A, Stoika I M and Vysochanskii Y M, 2003. Fast near-infrared self-pumped phase conjugation with photorefractive $Sn_2P_2S_6$. J. Opt. Soc. Amer. B. **20**: 1241–1256.
9. Mys O, Martynyuk-Lototska I, Grabar A and Vlokh R 2009. Acoustic and elastic properties of $Sn_2P_2S_6$ crystals. J. Phys.: Condens. Matter. **21**: 265401.
10. Haertle D, Guarino A, Hajfler J, Montemezzani G and Günter P, 2005. Refractive indices of $Sn_2P_2S_6$ at visible and infrared wavelengths. Opt. Express. **13**: 2047–2057.
11. Carpentier C D and Nitsche R, 1974. Vapour growth and crystal data of the thio(seleno) hypodiphosphates $Sn_2P_2S_6$, $Sn_2P_2Se_6$, $Pb_2P_2S_6$, $Pb_2P_2Se_6$ and their mixed crystals. Mat. Res. Bull. **9**: 401–410.
12. Dixon R W and Cohen M G, 1966. A new technique for measuring magnitudes of photoelastic tensors and its application to lithium niobate. Appl. Phys. Lett. **8**: 205–207.
13. Magdich L N and Molchanov V Ya. Acoustooptic devices and their applications. Gordon and Breach Science Publishing (1989).

Martynyuk-Lototska I., Dudok T., Mys O., Grabar A. and Vlokh R. 2019. Elasto-optic coefficients of $Sn_2P_2S_6$ crystals as determined with Dixon-Cohen method. Ukr.J.Phys.Opt. **20**: 54 – 59. doi: 10.3116/16091833/20/2/54/2019

Анотація. *За допомогою методу Діксона–Коена визначено набір еластооптичних коефіцієнтів і акустооптичних показників якості кристалів $Sn_2P_2S_6$. Розглянуто геометрію дифракції, пов'язану з акустооптичними взаємодіями із чисто поздовжньою акустичною хвилею, що поширюється вздовж кристалографічної осі b. Встановлено, що максимальний акустооптичний показник якості для цієї геометрії складає $(447\pm10)\times10^{-15}$ с^3/кг і досягається у випадку ізотропної взаємодії з оптичною хвилею, поляризованою паралельно до осі b.*